Studies of FeMn/Co/Cu(001) films using photoemission electron microscopy and surface magneto-optic Kerr effect

C. Won,[1] Y. Z. Wu,[1] H. W. Zhao,[1,2] A. Scholl,[3] A. Doran,[3] W. Kim,[1,4] T. L. Owens,[1] X. F. Jin,[5] and Z. Q. Qiu[1]
[1]*Department of Physics, University of California Berkeley, Berkeley, California 94720, USA*
[2]*International Center for Quantum Structures and State Key Laboratory for Magnetism, Institute of Physics, CAS, Beijing 100080, People's Republic of China*
[3]*Advanced Light Source, Lawrence Berkeley National Laboratory, Berkeley, California 94720, USA*
[4]*KRISS, Yuseong, Daejon, Republic of Korea*
[5]*Department of Physics, Fudan University, Shanghai, People's Republic of China*
(Received 14 September 2004; revised manuscript received 22 October 2004; published 12 January 2005)

FeMn/Co/Cu(001) films were epitaxially grown and investigated using photoemission electron microscopy and the surface magneto-optic Kerr effect. The FeMn antiferromagnetic order increases the Co film coercivity, switches the Co magnetization easy axis from the [110] direction to the [100] direction, and increases the Co film critical thickness at which the ferromagnetic transition occurs. The Néel temperature of the FeMn film increases with increasing FeMn film thickness. At room temperature, we constructed a magnetic phase diagram in the FeMn—Co thickness plane to describe the FeMn and Co magnetic phases.

DOI: 10.1103/PhysRevB.71.024406 PACS number(s): 75.70.Ak

The study of magnetic interactions at the interface of ferromagnetic (F) and antiferromagnetic (AF) materials has attracted much attention for several decades since the discovery of the exchange bias effect.[1] Rich phenomena have been reported in F/AF systems such as coercivity enhancements,[2] defect-induced disorder,[3] oscillatory exchange bias,[4] perpendicular exchange bias,[5] and step-induced spin frustration.[6] Different from the interfacial interactions between two ferromagnetic materials, the spin frustration at a F/AF interface plays a key role in determining the overall magnetic properties of the system.[7] Under certain conditions, the F/AF interfacial interaction is important even above the bulk Néel temperature of the antiferromagnetic material.[8] To obtain a better understanding of the F/AF interfacial interaction, x-ray magnetic linear dichroism (XMLD) has been applied to image AF domains and directly reveal the magnetic correlation at F/AF interfaces.[9] Also, single-crystalline ultrathin films have been synthesized to simplify the interfacial spin configurations at F/AF interfaces. High-quality FeMn/Co/Cu(100) thin films were recently synthesized and investigated.[10] It was shown that an FeMn single-crystal film can exhibit three-dimensional noncollinear antiferromagnetic order when sandwiched between two ferromagnetic films,[11] and that the Co film magnetic domains could be significantly affected at the FeMn antiferromagnetic transition.[12] These advances make it possible to futher single out the effect of F/AF interfacial interaction on the magnetic properties of F/AF systems. In this paper, we report the results of our study of the FeMn/Co/Cu(001) system using photoemission electron microscope (PEEM) and the surface magneto-optic Kerr effect (SMOKE). Using element-specific measurements, we construct a phase diagram to summarize the effect of F/AF interfacial interaction on the magnetic transitions of the FeMn and Co films. First, we find that the Co film, frustrated by the FeMn antiferromagnetic states, exhibits local uniaxial anisotropy which switches the Co magnetization easy axis from the [110] to the [100] direction. Second, the Néel temperature of the FeMn film increases with its thickness. Finally, we construct a phase diagram to describe the FeMn and Co magnetic transitions.

A Cu(001) single-crystal substrate was chemically polished and cleaned in vacuum by cycles of Ar ion sputtering at ~2 keV and annealing at ~600 °C. Co and FeMn films were epitaxially grown on to the Cu(001) substrate at room temperature. The vacuum pressure remained below $\sim 5 \times 10^{-10}$ Torr during the film growth. The FeMn alloy film was grown by coevaporating Fe and Mn with equal evaporation rate to achieve a 50-50 composition. The evaporation rate was monitored prior to the growth by a quartz thickness monitor which was calibrated by reflection high-energy electron diffraction intensity oscillations. The accuracy of the Fe and Mn composition ratio is controlled within 10%. The Co and FeMn films were grown into cross wedges by moving the Cu substrate behind a knife-edge shutter along two orthogonal directions [Fig. 1(a)]. The wedge slope (~3 monolayers (ML)/mm for Co and ~7 ML/mm for FeMn) is determined by the moving speed of the Cu substrate and the film growth rate. SMOKE measurements were performed *in situ* in both longitudinal and polar geometry. No polar signal was detected in the FeMn/Co/Cu(001) system, showing that the Co magnetization direction is in the plane of the film. For the PEEM experiment, a 15 ML Cu film was grown on the top of the sample to protect it from contamination. The sample was then transferred into the PEEM chamber at beamline 7.3.1.1 of the Advanced Light Source of the Lawrence Berkeley National Laboratory. The incident x-ray beam is circularly polarized and makes a 60° incident angle relative to the surface normal direction. Magnetic domain images were constructed by taking the ratio of L_3 and L_2 edges utilizing the effect of x-ray magnetic circular dichroism (XMCD).[13]

Since XMLD has not been successfully applied to metallic antiferromagnetic materials, it is impossible to measure directly the antiferromagnetic order of an FeMn film.[10] How-

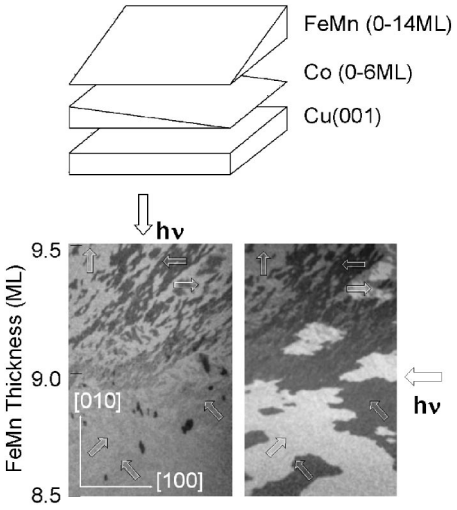

FIG. 1. (a) Schematic drawing of the FeMn/Co double wedges grown on Cu(001). (b) Room-temperature domain images of Co film in FeMn/Co(4 ML)/Cu(001). Arrows inside the images show the Co local magnetization directions. Arrows outside the images indicate the direction of the incident x ray. Each PEEM image covers a sample area of 40 μm$\times$60 μm. The Co easy magnetization axis switches from [110] to [100] at ~9.0 ML of FeMn where the FeMn film establishes its antiferromagnetic order at room temperature.

ever, Kuch *et al.*[10] showed that the FeMn antiferromagnetic order in the FeMn/Co/Cu(001) system can be revealed indirectly by domain images of the ferromagnetic Co film. Upon doing so, the Co magnetic domains break into small-sized domains as the FeMn film establishes its antiferromagnetic order. In addition, the Co magnetization easy axis switches from the [110] direction in the paramagnetic state of the FeMn film to the [100] direction in the antiferromagnetic state of the FeMn film. Note that the local Co domain intensity in the PEEM measurement is proportional to the projection of the Co magnetization on the incident x-ray beam direction. Thus the local Co magnetization direction can be determined by comparing two PEEM images taken at two different incident directions of the x-ray beam.[10] Figure 1(b) shows two Co domain images of FeMn/Co(4 ML)/Cu(001) taken with the in-plane projection of the incident x-ray beam parallel to the $[\bar{1}00]$ and $[0\bar{1}0]$ crystalline directions. Under this measurement geometry, the PEEM image of the Co film should consist of two different domain intensities for the [110] magnetization easy axis and three different domain intensities for the [100] magnetization easy axis. Then the local Co magnetization direction [indicated by arrows in Fig. 1(b)] can be easily determined by comparing the two PEEM images of Fig. 1(b). It is clearly seen that the Co magnetization easy axis switches from the [110] direction below 9 ML FeMn to the [100] direction above 9 ML FeMn. In addition, the Co domain size experiences a sudden change at 9 ML FeMn. Therefore, the result of Fig. 1(b) confirms the conclusion of Ref. 10 that the FeMn film establishes its antiferromagnetic order at ~9 ML and that the FeMn antiferromagnetic state switches the Co magnetization easy axis to the [100] direction.

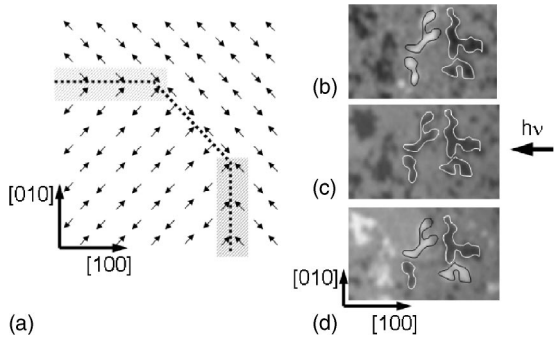

FIG. 2. (a) Schematic drawing of the spin configuration of a FeMn(001) surface with a monolayer-high island. The dotted line shows the island boundary. Co domain images (8 μm$\times$6 μm) of FeMn(11 ML)/Co(3.5 ML)/Cu(001) (b) in the as-grown state, (c) after applying a ~1 kOe magnetic pulse along the $[\bar{1}00]$ direction, and (d) after demagnetizing the sample with a 60 Hz ac magnetic field along the [100] direction.

The Co [100] magnetization easy axis in FeMn/Co/Cu(001) at the antiferromagnetic state of FeMn can be understood in terms of the FeMn spin structure. It is known that FeMn has a 3*Q*-like spin structure[14,15] so that the in-plane spin projection of FeMn(001) sheets alternates from the $\pm[110]$ to the $\pm[1\bar{1}0]$ direction between adjacent sheets. Although each FeMn(001) plane is a spin-compensated plane, an atomic step parallel to the [100] or [010] direction on an FeMn(001) surface could result in an uncompensated magnetic moment in the $\pm$[100] or $\pm$[010] direction, while a step parallel to the [110] direction would not induce an uncompensated moment [Fig. 2(a)]. Then a direct coupling of the Co magnetic moment to the FeMn uncompensated moment at the [100] steps explains the Co [100] magnetization easy axis in the antiferromagnetic state of FeMn [11]. The above anisotropy mechanism should generate a uniaxial or unidirectional magnetic anisotropy whose local easy axis varies randomly in space. This is very different from the conventional fourfold in-plane magnetocrystalline anisotropy for a (001) film which generates four energetically equivalent magnetization easy axes. Since an as-grown Co(001) film could develop magnetic domains with four possible magnetization directions, the Co domains shown in Fig. 1(b) cannot be used to distinguish between the uniaxial/unidirectional anisotropy and the fourfold magnetocrystalline anisotropy. To explore the nature of the Co [100] magnetization easy axis, we applied an external magnetic field pulse (~1 kOe) to the FeMn(11 ML)/Co(3.5 ML)/Cu(001) along the $[\bar{1}00]$ direction and measured the Co magnetic domains with the in-plane projection of the incident x-ray beam along the $[\bar{1}00]$ direction. The Co domain intensity under this measurement geometry should be white, dark, and gray for magnetization along the [100], $[\bar{1}00]$, and $\pm$[010] directions, respectively. If the Co [100] magnetization direction in the FeMn/Co/Cu(001) system were determined by a fourfold magnetic anisotropy, the application of the magnetic pulse would switch all magnetic domains into the magnetic field direction, leading to a single-domain PEEM image. By com-

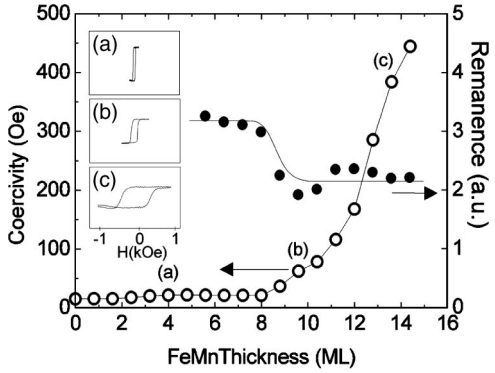

FIG. 3. Coercivity and remanence of FeMn/Co(6.5 ML)/Cu(001) from SMOKE measurements with the magnetic field applied along the [110] axis. The insets of (a), (b), and (c) show the hysteresis loops at the indicated FeMn thicknesses. The FeMn film establishes its antiferromagnetic order at ~9 ML.

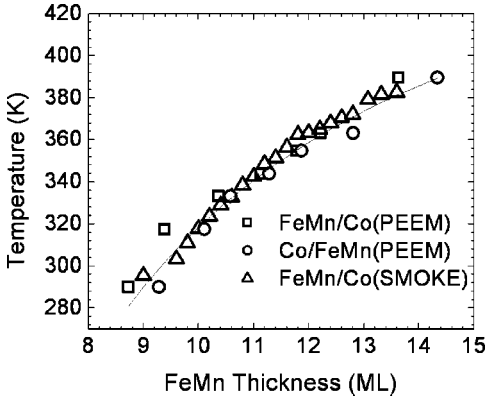

FIG. 4. FeMn Néel temperature of FeMn/Co(4 ML) films grown on Cu(001). The first two data sets (squares and circles) are from PEEM measurements. The last data set (triangles) is from SMOKE measurements. Solid line depicts the fitting result using Eq. (1).

paring the Co domain intensities before [Fig. 2(b)] and after [Fig. 2(c)] the magnetic pulse, it is clear that only the Co domains with [100] magnetization switch to the $[\bar{1}00]$ direction after the magnetic pulse, and the domains with ±[010] magnetizations remain in the ±[010] directions. Noting that ±[010] magnetizations are perpendicular to the magnetic pulse direction, the results of Fig. 2(b) and 2(c) show that it is energetically unstable to rotate the magnetization to the perpendicular direction of the local easy axis. This result indicates that the local Co [100] easy magnetization axis in the FeMn/Co/Cu(001) is not from a conventional fourfold magnetic anisotropy, but from a local uniaxial or unidirectional magnetic anisotropy whose easy axis alternates randomly in space between the ±[100] and ±[010] directions. To further confirm the uniaxial or unidirectional nature of the [100] easy magnetization axis, we demagnetized the sample by gradually reducing the amplitude of a 60 Hz ac magnetic field in the [100] direction. The Co domains after the demagnetization [Fig. 2(d)] show again that those domains with their magnetizations perpendicular to the demagnetization field remain unchanged, supporting the uniaxial or unidirectional nature of the magnetic anisotropy. In addition, we found that Co domains with [100] or $[\bar{1}00]$ magnetization could flip their magnetic directions after demagnetization, showing that the local magnetic anisotropy is dominated by uniaxial anisotropy rather than by unidirectional anisotropy, that is, the local coercivity should be greater than the local exchange bias.

The existence of the local uniaxial or unidirectional magnetic anisotropies should have a significant effect on the Co magnetization switching. This was indeed confirmed by *in situ* SMOKE measurements on FeMn/Co(6.5 ML)/Cu(001). Figure 3 shows the coercivity and remanence of the 6.6 ML Co film from longitudinal SMOKE measurement with the magnetic field applied along the [110] direction. Representative hysteresis loops at three different FeMn film thicknesses are show in the inset of Fig. 3. We found that the Co coercivity exhibits a drastic increase as the FeMn thickness increases to establish antiferromagnetic order at ~9 ML FeMn: the Co coercivity increases from ~20 Oe below 8 ML FeMn to ~400 Oe above 14 ML FeMn, and meanwhile the magnetic remanence decreases due to the switching of the easy magnetic axis from the [110] to [100] directions. Unfortunately we could not rotate the sample by 45° in our UHV system so that we did not obtain hysteresis loops of the Co film for magnetic field applied along the [100] direction. Such measurement could add valuable data to the analysis. Because our SMOKE magnetic can only reach ~1–1.5 kOe magnetic field, we also could not obtain the saturation field of the hysteresis loops at thicker FeMn. The saturation field may provide indirect information on the FeMn-induced magnetic anisotropy. Obviously, more detailed measurements are needed in the future. It should be mentioned that a coercivity enhancement also exists in the MnF_2/Fe system below the MnF_2 Néel temperature, and this effect was attributed to the magnetic interfacial frustration.[2] Since the local uniaxial or unidirectional magnetic anisotropy comes from the FeMn atomic steps along the [100] or [010] directions, a complete understanding of the local magnetic anisotropy requires detailed information on the local FeMn/Co interfacial morphology. This could be a future project for a scanning tunneling microscopy experiment.

We now turn our attention to the FeMn paramagnetic-to-antiferromagnetic transition. Since the FeMn antiferromagnetic transition in FeMn/Co/Cu(001) system can be determined by both PEEM and SMOKE measurements on the Co film, we studied the thickness dependence of the FeMn Néel temperature in FeMn/Co(4 ML)/Cu(001) and Co(4 ML)/FeMn/Cu(001). The sample temperature was increased gradually, and at each temperature the FeMn phase transition critical thickness was determined experimentally (Fig. 4). We found that the FeMn Néel temperature increases with film thickness and is almost identical for FeMn/Co/Cu(001) and Co/FeMn/Cu(001). We also found that the FeMn Néel temperature depends very little on Co film thickness once the Co film is in the ferromagnetic state. Lowered Néel temperature in an antiferromagnetic thin film has been reported in the literature,[16,17] and was attributed to a finite-size effect. Previous studies were usually limited to a few thicknesses of the antiferromagnetic film. The applica-

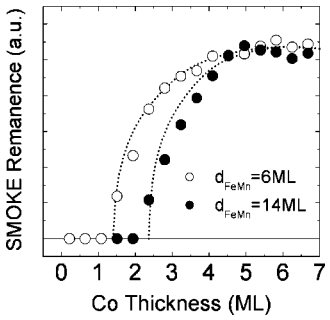

FIG. 5. Magnetic remanence of FeMn/Co/Cu(001) determined from SMOKE measurements. The dotted lines are to guide the eye.

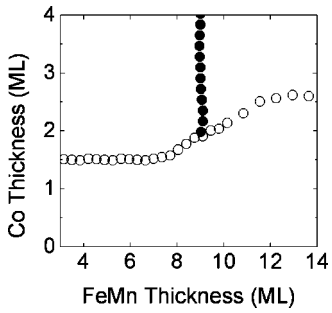

FIG. 6. Phase diagram of FeMn/Co/Cu(001) at room temperature. The open dots define the Co critical thickness and solid dots define the FeMn critical thickness. Note that the FeMn critical thickness cannot be determined in our experiment below the Co critical thickness.

tion of a wedged sample in the present work enables a detailed study of the thickness dependence of the Néel temperature. The finite-size effect in magnetic phase transitions is usually described by a scaling law of

$$\frac{T(\infty) - T(n)}{T(\infty)} \approx \left(\frac{n_0}{n}\right)^{\lambda}, \tag{1}$$

where $T(\infty)$ is the critical temperature in the bulk limit, n is the film thickness, and λ is a critical exponent whose value reflects the universality class of the phase transition.[18] Using the bulk value (500 K) of the FeMn Néel temperature,[19] we fitted the experimental data (solid line in Fig. 4) and obtained $\lambda = 1.38 \pm 0.04$ and $n_0 = 4.8 \pm 0.1$. Although the fitting agrees reasonable well with the experimental data, the justification of using Eq. (1) is a topic of discussion. First, it is questionable if Eq. (1) can be applied directly to an antiferromagnetic film in a coupled system (e.g., FeMn/Co bilayers). Second, it was shown recently that Eq. (1) needs to be modified in the ultrathin film regime, which could significantly change the λ value.[20] The above concerns make us conservative in attempting to interpret the λ value. Nevertheless, we here provide the fitting result, aiming to stimulate theoretical interest to this topic.

Because a compensated antiferromagnetic surface consists of spins that alternate their directions over an atomic scale, a ferromagnetic thin film coupled to a compensated antiferromagnetic surface should exhibit a different magnetic phase transition from that of a single ferromagnetic film. We now discuss the effect of the antiferromagnetic FeMn on the Co ferromagnetic transition in FeMn/Co/Cu(001). The Curie temperature (T_C) of a magnetic film is usually determined from the temperature dependence of the magnetization. Since the T_C of a magnetic film increases with film thickness, a thickness-dependent magnetic measurement at a fixed temperature could determine a critical thickness whose T_C is equal to the measurement temperature.[13] Experimentally, a thickness-dependent measurement is easier to perform than a temperature-dependent measurement for a wedged samples. We performed SMOKE measurements at room temperature on an FeMn/Co(wedge)/Cu(001) sample to obtain the thickness-dependent magnetic remanence of the Co film. Figure 5 shows the results from FeMn(6 ML)/Co/Cu(001) and FeMn(14 ML)/Co/Cu(001). For each sample, the magnetic remanence develops rapidly above a critical thickness to approach a saturation value, showing a magnetic transition at the critical thickness. However, the Co critical thickness of FeMn(14 ML)/Co/Cu(001) is greater than the Co critical thickness of FeMn(6 ML)/Co/Cu(001). Recall that the T_C of a magnetic film increases with film thickness and that the FeMn film establishes its antiferromagnetic order above ~9 ML thickness; thus the thicker Co critical thickness of FeMn(14 ML)/Co/Cu(001) indicates that the FeMn antiferromagnetic order reduces the T_C of the Co film. We also took Co PEEM images at room temperature along the Co wedge in FeMn/Co/Cu(001) and determined the Co critical thickness where the magnetic domain contrast disappears. To ensure that the Co film below the critical thickness is not in a single-domain ferromagnetic state, we took x-ray absorption spectra of the Co film below the critical thickness using left- and right-circularly-polarized incident x rays and found no XMCD signal, so the Co film below the critical thickness is not in the ferromagnetic state. Figure 6 shows the Co critical thickness (open dots) determined at different FeMn thicknesses. Below 8 ML FeMn, the Co critical thickness remains at a constant value of ~1.5 ML, which is similar to the critical thickness of a Co film on Cu(001). Since FeMn is in the paramagnetic state below 9 ML, the constant Co critical thickness below 8 ML FeMn shows that the paramagnetic phase of FeMn has little effect on the Co ferromagnetic order. As the FeMn thickness increases from 8 ML, the Co critical thickness increases gradually to 2.5 ML and remains a constant value of 2.5 ML for FeMn films thicker than 12 ML. It should be mentioned that the absence of the Co XMCD signal below the Co critical thickness only proves that Co is not in the ferromagnetic state, but we cannot rule out the possibility of the existence of another magnetic state than the paramagnetic state (such as a spin-glass state). To a certain extent, the magnetic coupling at an F/AF interface can be viewed as applying a random magnetic field to the ferromagnetic film. The effect of a random magnetic field on a ferromagnetic system has been investigated extensively in theory.[21,22] Some simple models, such as the random field Ising model, were also developed to address the phase transition issue,[23–25] The results shown in Fig. 6 are related to this subject. In Fig. 6, from PEEM images, we plotted the FeMn transition boundary (solid circles) where domain frustration starts as shown in Fig. 1. We found that the FeMn

critical thickness depends very little on the Co thickness above the Co critical thickness (where Co is in the ferromagnetic state). Below the Co critical thickness, we could not determine the FeMn critical thickness due to the absence of the Co magnetic domains. Obviously, there should exist a FeMn boundary that defines the FeMn antiferromagnetic transition. It would be very interesting to find out in the future whether or not the FeMn critical thickness would be increased or decreased by the ferromagnetic state of the Co film.

In summary, we investigated the effect of F/AF interactions on the magnetic properties of FeMn/Co/Cu(001) using PEEM and SMOKE. The FeMn antiferromagnetic order switches the Co magnetization easy axis to the [100] direction and increases the Co coercivity. These results are attributed to step-induced local uniaxial or unidirectional magnetic anisotropy whose direction varies randomly in space. FeMn and Co magnetic transitions were also explored by constructing a magnetic phase diagram in the FeMn—Co thickness plane. We find that the FeMn antiferromagnetic order has the effect of increasing the Co transition critical thickness.

This work was supported by National Science Foundation Grant No. DMR-0405259, U.S. Department of Energy Grant No. DE-AC03-76SF00098, the Chinese National Science Foundation, the Chinese Science and Technology Ministry for 973 Project, and ICQS of CAS.

[1] W. H. Meiklejohn and C. P. Bean, Phys. Rev. **102**, 1413 (1956).
[2] C. Leighton, J. Nogués, B. J. Jönsson-Åkerman, and I. K. Schuller, Phys. Rev. Lett. **84**, 3466 (2000).
[3] P. Miltényi, M. Gierlings, J. Keller, B. Beschoten, G. Güntherodt, U. Nowak, and K. D. Usadel, Phys. Rev. Lett. **84**, 4224 (2000).
[4] F. Y. Yang and C. L. Chien, Phys. Rev. Lett. **90**, 147201 (2003).
[5] S. Maat, K. Takano, S. S. P. Parkin, and E. E. Fullerton, Phys. Rev. Lett. **87**, 087202 (2001).
[6] U. Schlickum, N. Janke-Gilman, W. Wulfhekel, and J. Kirschner, Phys. Rev. Lett. **92**, 107203 (2004).
[7] J. Nogués and Ivan K. Schuller, J. Magn. Magn. Mater. **192**, 203 (1999).
[8] M. Grimsditch, A. Hoffmann, P. Vavassory, Hongtao Shi, and D. Lederman, Phys. Rev. Lett. **90**, 257201 (2003).
[9] H. Ohldag, T. J. Regan, J. Stöhr, A. Scholl, F. Nolting, J. Lüning, C. Stamm, S. Anders, and R. L. White, Phys. Rev. Lett. **87**, 247201 (2001).
[10] W. Kuch, F. Offi, L. I. Chelaru, M. Kotsugi, K. Fukumoto, and J. Kirschner, Phys. Rev. B **65**, 140408 (2002).
[11] F. Offi, W. Kuch, L. I. Chelaru, K. Fukumoto, M. Kotsugi, and J. Kirschner, Phys. Rev. B **67**, 094419 (2003).
[12] Wolfgang Kuch, Liviu I. Chelaru, Francesco Offi, Jing Wang, Masato Kotsugi, and Jürgen Kirschner, Phys. Rev. Lett. **92**, 017201 (2004).
[13] C. Won, Y. Z. Wu, A. Scholl, A. Doran, N. Kurahashi, H. W. Zhao, and Z. Q. Qiu, Phys. Rev. Lett. **91**, 147202 (2003).
[14] G. Malcolm Stocks, W. A. Shelton, Thomas C. Schulthess, Balazs Ujfalussy, W. H. Butler, and A. Canning, J. Appl. Phys. **91**, 7355 (2002).
[15] H. Umebayashi and Y. Ishikawa, J. Phys. Soc. Jpn. **21**, 1281 (1966).
[16] T. Ambrose and C. L. Chien, Phys. Rev. Lett. **76**, 1743 (1996).
[17] D. Alders, L. H. Tjeng, F. C. Voogt, T. Hibma, G. A. Sawatzky, C. T. Chen, J. Vogel, M Sacchi, and S. Iacobucci, Phys. Rev. B **57**, 11 623 (1988).
[18] Douglas S. Ritchie and Michael E. Fisher, Phys. Rev. B **7**, 480 (1973).
[19] H. Umebayashi and Y. Ishikawa, J. Phys. Soc. Jpn. **21**, 1281 (1966); J. H. Smith, J. Appl. Phys. **39**, 675 (1968).
[20] Renjun Zhang and Roy F. Willis, Phys. Rev. Lett. **86**, 2665 (2001).
[21] Yoseph Imry and Shang-keng Ma, Phys. Rev. Lett. **35**, 1399 (1975); G. Grinstein, *ibid.* **37**, 944 (1976).
[22] G. Grinstein and Shang-keng Ma, Phys. Rev. B **28**, 2588 (1983).
[23] For a review, see D. P. Belanger and A. P. Young, J. Magn. Magn. Mater. **100**, 272 (1991).
[24] Amnon Aharony, Phys. Rev. B **18**, 3318 (1978).
[25] K. Binder, Phys. Rev. B **29**, 5184 (1984).